ISBN: 978-3-95450-261-5 ISSN: 2673-7000 doi: 10.18429/JACoW-NAPAC2025-TUP093

START-TO-END SIMULATION STUDY FOR TRANSVERSE WIGGLER-BASED MANIPULATION EXPERIMENT

G. Ha* and D. Sinha, Northern Illinois University, DeKalb, USA

Content from this work may be used under the terms of the CC BY 4.0 licence (© 2025). Any distribution of this work must maintain attribution to the author(s), title of the work, publisher, and DOI.

Abstract

We present a simulation study to support the planning of experimental demonstrations of transverse wiggler-based correlation control. While previous simulations confirmed the feasibility of this approach, they did not incorporate realistic field maps of the transverse wigglers. In addition, the impact of various jitter and error sources—key concerns for experimental implementation—has not been analyzed. In this study, wiggler fields are generated through magnetostatic simulations and incorporated into start-to-end particle tracking simulations. The phase space responses to different jitter and error sources are also evaluated.

INTRODUCTION

Authors recently proposed a concept for tailoring phase space correlations for various applications [1]. The proposed method utilizes cosine modulation that can be generated by various tools, such as transverse wiggler [2], wakefield structure, or laser. Unlike conventional methods using multipole magnets, which provide a polynomial approximation of the desired correlation, this approach approximates the correlation using cosines, which significantly improves the quality and expands capability. Several simulations have been carried out to confirm the feasibility of the method and its applications [1, 3–6].

Later, we studied the expected side effects of a transverse wiggler [7], which could significantly limit its applicability to high-energy beams or other particles (e.g., protons or muons). This work considered three major limiting factors: (1) transverse wiggler thickness, (2) the dependence of B_y field on the particle's vertical position, and (3) the B_x field along the horizontal direction. The study concluded that (1) and (3) are negligible unless the manipulation requires extreme conditions. Also, a vertical beam size of 3-5% of the wavelength can almost eliminate the impact of (2).

As the next step toward preparing an experimental demonstration, we performed another simulation study to examine the manipulation method's sensitivity to errors. We discuss issues found during start-to-end simulations, as well as the sensitivity of the manipulation to transverse wiggler parameters and injector parameters.

START-TO-END SIMULATION

The simulation was performed using the General Particle Tracer GPT code [8]. The Argonne Wakefield Accelerator facility [9] was modeled in GPT, and four accelerating columns were used to produce a 44-MeV electron beam. The layout of the beamline and corresponding beam envelope are shown in in Fig. 1. The bunch charge was set to 1 nC for the simulation. The downstream of the linac includes two sets of quadrupole triplet followed by transverse wigglers. To minimize the impact from $B_y(y)$ field components, vertical focusing is necessary while the horizontal beam size should be enlarged to avoid the use of short-period wigglers. Two sets were originally prepared to enable both shaping to a doorstep profile and linearization of the phase space downstream. The transverse wigglers placed at position **A** were optimized to generate a doorstep profile at position **B**. We ignore the linearization part in this paper.

Seven wigglers were used to optimize the phase space for generating the doorstep profile. A differential evolution algorithm was employed to search for optimal period combinations while the corresponding amplitudes and phases were calculated via linear regression. This combined approach can significantly reduce optimization time from a few days to a few hours. However, further R&D on the optimization and online tuning is necessary [10]. The periods and wiggler gaps are summarized in Table 1. For simplicity, cube magnets with dimensions of $\lambda/4 \times \lambda/4 \times \lambda/4$ were assumed to form a Halbach array [11].

Table 1: Transverse Wiggler Parameters

Wiggler index	Periods (mm)	Gap (mm)
1	29.60	15.96
2	21.20	14.03
3	13.30	31.61
4	10.40	10.89
5	7.10	11.00
6	6.30	10.07
7	5.60	21.92

Figure 2 shows the horizontal phase spaces before and after the transverse wigglers, as well as after transport to position **B**. This calculation assumes ideal kicks from the transverse wigglers. The resulting horizontal phase space at position **B** shows the designed doorstep profile, which starts at +5 mm and ends at -5 mm with a rectangular step spanning from +3.5 mm to +5.0 mm.

We also simulated the transverse wigglers with imported 3D field maps. Figure 3 shows a comparison of horizontal phase spaces at both positions and the corresponding profiles at the end. Panel (a) shows that the result obtained with 3D field maps resembles the ideal case. However, the result from the 3D field map also contains numerous artifacts originating from simulation accuracy and possibly harmonics components. These artifacts introduce significant deformation in the density profile as shown in Fig. 3 (b). Follow-up studies will be conducted.

* gha@niu.edu

ISBN: 978-3-95450-261-5 ISSN: 2673-7000 doi: 10.18429/JACoW-NAPAC2025-TUP093

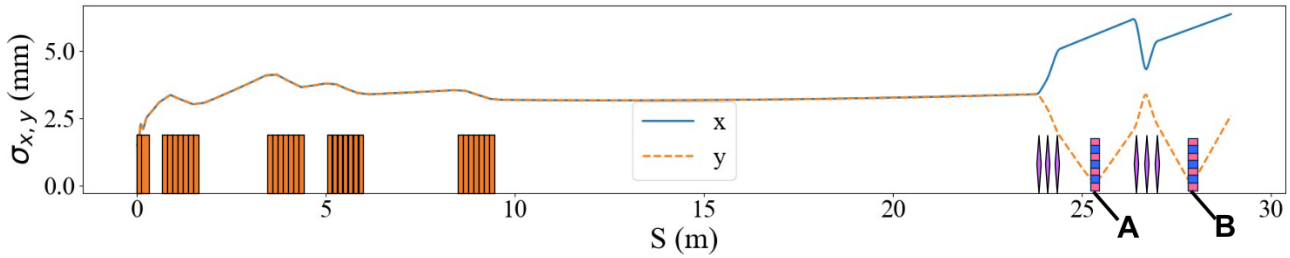

Figure 1: Beamline layout with beam envelopes. Brown boxes, purple diamonds, and boxes with alternating colors represent accelerating columns, quadrupoles, and transverse wigglers, respectively.

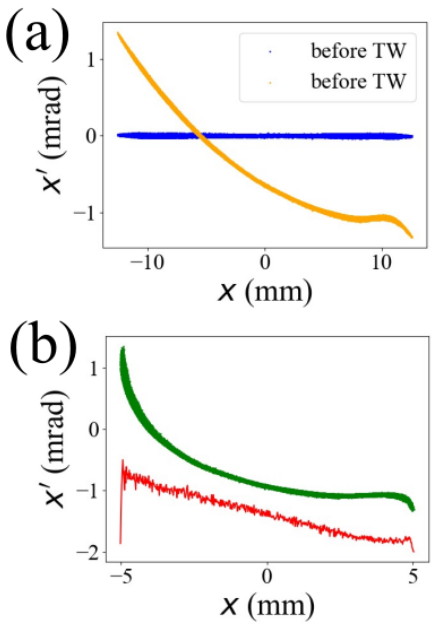

Figure 2: Horizontal phase space and corresponding x-profile. (a) Horizontal phase space before and after a set of transverse wigglers placed at position **A**. (b) Horizontal phase space at position **B** and its corresponding horizontal profile.

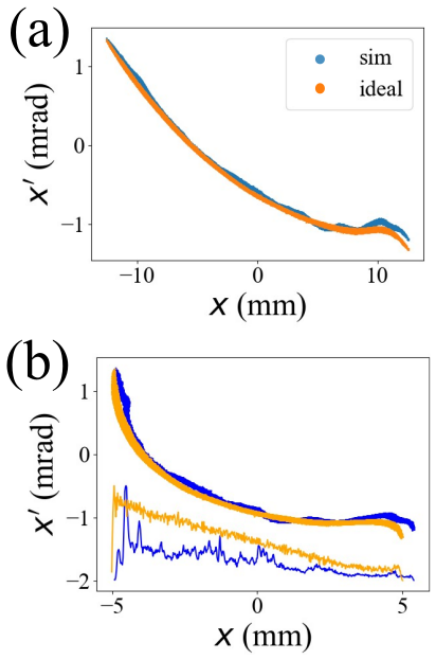

Figure 3: Comparison of ideal and simulated transverse wigglers. (a) horizontal phase spaces after a set of transverse wigglers at position **A**. Color corresponds to ideal transverse wiggler case and simulated wiggler case. (b) horizontal phase spaces at position **B** and corresponding horizontal profiles.

MANIPULATION TOLERANCE: WIGGLER PARAMETERS

While the method can tailor the correlation quite accurately with ideal wigglers, such high accuracy also means the methods could be vulnerable to errors. We applied random errors to three of wiggler parameters converted to engineering scales: period, wiggler gap size, offset in x-direction. Two quantities were used as indicators of the deviations. One is the transformer ratio with an assumption of wavelength roughly matched to the ideal profile, and the other is the standard deviation of the correlation differences at each data point. Ideal wigglers were used for this test.

The range of random errors were set to ± 5, ± 10, ± 25, and ± 50 µm. Each error has a uniform probability of taking any values within the range. Figure 4 summarizes the results for (i) errors on period only, (ii) errors on gap size only, (iii) errors on offsets only, and (iv) errors on all parameters simultaneously. One thousand error sets were tested for each case.

Interestingly, each wiggler parameter had a similar impact on both transformer ratio and the correlation difference although the actual correlation shapes differed slightly. For correlations, errors slightly over 20 µm were acceptable for individual parameters, and 20 µm was the maximum tolerable error range when all errors were combined. The transformer ratio, however, was much more sensitive. Roughly 20 µm was tolerable for individual parameters while only 10 µm was allowable when all errors were combined.

The results indicate two main points. First, the three transverse wiggler parameters—period, gap, and offset—should be controlled within a 10 µm range. This is a challenging requirement for the period. While such accuracy is relatively easy to achieve for the gap and the offset, it suggests that an

Content from this work may be used under the terms of the CC BY 4.0 licence (© 2025). Any distribution of this work must maintain attribution to the author(s), title of the work, publisher, and DOI.

ISBN: 978-3-95450-261-5 ISSN: 2673-7000 doi: 10.18429/JACoW-NAPAC2025-TUP093

© Content from this work may be used under the terms of the CC BY 4.0 licence (© 2025). Any distribution of this work must maintain attribution to the author(s), title of the work, publisher, and DOI.

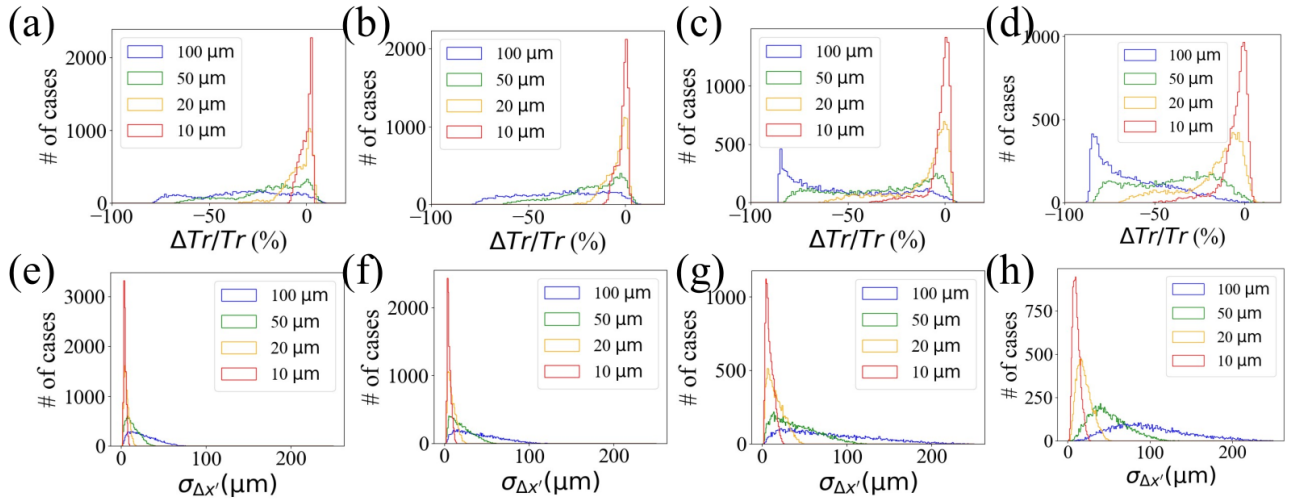

Figure 4: Error test results for wiggler parameters. (a-d) show the transformer ratio responses to errors. (e-h) show the standard deviation of correlation differences for various error cases. Each column corresponds to: period error only, gap size error only, offset error only, and all error combined, respectively.

automated tuning algorithm to control seven wigglers will be necessary. Second, the tolerance could be differ significantly for individual applications.

MANIPULATION TOLERANCE: INJECTOR PARAMETERS

Similar to the previous section, we also carried out tolerance tests for injector parameters. Due to the large number of parameters in injector, this preliminary study was limited to a few simple test cases. Only individual error sources were tested, one at a time. The matching solenoid strength was varied from -4 A to +4 A relative to its original setting with 1 A steps. The laser radius was varied from -0.4 mm to 0.4 mm with 0.1 mm steps. All cavity voltages were varied from -0.4% to +0.4% of the original setting with 1%p steps. Finally, all cavity phases were varied from –4° to +4° from the original setting with 1° steps.

The results shown in Fig. 5 indicates that a range of ±2 [unit] reasonably preserves the profile. Impact of the energy change is relatively smaller than that of the changes in the beam size. Although the corresponding figure is not provided in this paper, these errors primarily distort the head and tail of the final profile.

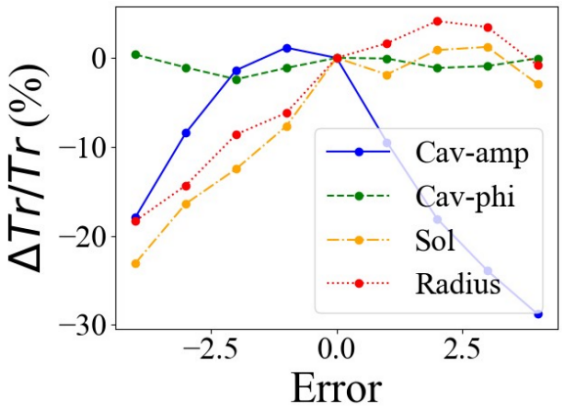

Figure 5: Transformer ratio response to injector parameter errors.

SUMMARY

We performed start-to-end simulations and manipulation tolerance tests. The start-to-end simulation with idealized wigglers provided the designed correlation and density profiles at the defined location. Similarly, simulations using wiggler field maps yielded a correlation comparable to the ideal case, but with numerous artifacts that significantly distorted the final density profile. These distortions may result from both simulation accuracy and higher-order magnet components, and further investigation is required. Tolerance tests for wiggler and injector parameters were carried out using idealized wiggler kicks. The results indicated that 10 μm-level accuracy is required for controlling the period, gap size, and the offset. In addition, errors within ±2 [unit] for focusing solenoid strength, laser radius, cavity amplitude, and cavity phase produced only tolerable deformation of the final density profile.

REFERENCES

[1] G. Ha, "Arbitrary transverse and longitudinal correlation generation using transverse wiggler and wakefield structures", in *Proc. IPAC'23*, Venice, Italy, May 2023, pp. 2759–2762. doi:10.18429/JACoW-IPAC2023-WEPA045

[2] G. Ha, M. E. Conde, J. G. Power, J. H. Shao, and E. E. Wisniewski, "Tunable Bunch Train Generation Using Emittance Exchange Beamline With Transverse Wiggler", in *Proc. IPAC'19*, Melbourne, Australia, May 2019, pp. 1612–1614. doi:10.18429/JACoW-IPAC2019-TUPGW089

[3] G. Ha, "Emittance exchange with periphery cut for high-brightness beam", in *Proc. IPAC'23*, Venice, Italy, May 2023,

ISBN: 978-3-95450-261-5 ISSN: 2673-7000 doi: 10.18429/JACoW-NAPAC2025-TUP093

pp. 2763–2766.
doi:10.18429/JACoW-IPAC2023-WEPA046

[4] G. Ha and N. Majernik, "Generation of sawtooth correlation for bunching factor enhancement", in *Proc. IPAC'24*, Nashville, TN, May 2024, pp. 380–383. doi:10.18429/JACoW-IPAC2024-MOPG38

[5] G. Ha, "Imparting arbitrary correlation on longitudinal phase space using transverse wigglers and deflecting cavities", in *Proc. IPAC'24*, Nashville, TN, pp. 844–847, 2024. doi:10.18429/JACoW-IPAC2024-MOPS56

[6] A. D. G. Ha and B. T. Ozdemir, "Deflecting cavity-based multifunctional longitudinal manipulator for csr-mitigated bunch compression", Taipei, Taiwan, May 2025, paper TUPM014, to be published.

[7] G. Ha, "Study for limiting factors in transverse wiggler-based arbitrary correlation generation", in *Proc. IPAC'25*, Taipei, Taiwan, May 2025, paper WEPS023, to be published.

[8] Pulsar Physics, *General particle tracer (gpt)*, Pulsar Physics. https://www.pulsar.nl/gpt

[9] M. E. Conde *et al.*, "Research Program and Recent Results at the Argonne Wakefield Accelerator Facility (AWA)", in *Proc. IPAC'17*, Copenhagen, Denmark, May 2017, pp. 2885–2887. doi:10.18429/JACoW-IPAC2017-WEPAB132

[10] A. D. D. Wang and G. Ha, "Enabling arbitrary correlations in beam phase space via curve matching", in *Proc. IPAC'25*, Taipei, Taiwan, May 2025, paper THPS098, to be published.

[11] K. Halbach, "Application of permanent magnets in accelerators and electron storage rings", *J. Appl. Phys.*, vol. 57, p. 3605, 1985. doi:10.1063/1.335021

Content from this work may be used under the terms of the CC BY 4.0 licence (© 2025). Any distribution of this work must maintain attribution to the author(s), title of the work, publisher, and DOI.